Spin polarized tunneling as a probe for quantitative analysis of field dependent domain structure in magnetic tunnel junctions

C. Tiusan[a)]
Institut de Physique et de Chimie des Matériaux de Strasbourg, 23 rue du Loess, F-67037 Strasbourg Cedex, France

M. Hehn
Laboratoire de Physique des Matériaux, UMR CNRS 7556, BP 239, 54506 Vandoeuvre lès Nancy Cedex, France

T. Dimopoulos and K. Ounadjela
Institut de Physique et de Chimie des Matériaux de Strasbourg, 23 rue du Loess, F-67037 Strasbourg Cedex, France

Micromagnetic features appearing during the reversal of an artificial ferrimagnet used as a hard layer of a magnetic tunnel junction are quantitatively analyzed using the high sensitivity of the spin polarized tunnel current to magnetization fluctuations in the electrodes of the magnetic junctions. We propose an analytical model which takes into account different tunneling paths associated with local magnetization configurations. The model allows a quantitative correlation between the spin polarized transport characteristics and the field-dependent domain structure. The results extracted from the tunnel magnetoresistance measurements are found to be in good agreement with the magnetic domain wall density extracted from magnetic force microscopy experiments. © *2001 American Institute of Physics.* [DOI: 10.1063/1.1361044]

Micromagnetic domain structures within the ferromagnetic layers have been shown to have a large effect on the transport properties of the hard/soft magnetic tunnel junction (MTJ) architecture.[1–6] The understanding as well as the control of the magnetization reversal in the magnetic electrodes is the key parameter for optimizing the field response of the microelectronic devices. We present here a powerful technique for quantitatively investigating field-dependent micromagnetic features in thin magnetic layers. The technique uses the extreme sensitivity of the spin polarized tunneling in MTJs to the local magnetic configuration of each magnetic layer in contact with the tunnel barrier. The investigated magnetic layer is used as a magnetically hard electrode and it acts as a spin polarizer. The electrons which tunnel across the insulating layer are then analyzed by the magnetically soft electrode. We have used this technique for a quantitative study of the micromagnetic reversal mechanism in an artificial ferrimagnetic system (AFi), widely used nowadays as a hard subsystem in magnetic devices. The studied AFi is composed of a Co (2 nm)/Ru (0.8 nm)/CoFe (3 nm) trilayer separated by a 1 nm thick Al oxide barrier from the Co (1 nm)/Fe (6 nm) magnetically soft bilayer or detection layer (DL).[5,7] In the present work, the CoFe (3 nm) layer is interfaced with the barrier. We have developed an appropriate analytical model to demonstrate the use of the TMR signal as a probe for investigating the field dependent domain wall density and the average angle of domain magnetization. These values extracted from the TMR measurements are found to be in good agreement with the magnetic domain wall images analysis.

A typical magnetization versus field, $M-H$ curve, correlated with a tunnel magnetoresistance versus field, TMR$-H$ curve, for a Co/Ru/CoFe AFi based junction is shown in Fig. 1(a). The curves are measured in a ± 1 kOe field window where the AFi behaves as a single block of reduced moment $(M_1 - M_2)$ due to the strong antiferromagnetic coupling between its magnetic layers M_1 and M_2. We analyze Fig. 1(a) starting from positive maximum field. In a positive field the AFi net moment and the DL are parallel leading to a minimum value of the resistance. When reversing the external field, the DL switches at a field of about -30 Oe, illustrated in Fig. 1(a) by the drop (jump) in the $M-H$ (TMR) curve. The antiparallel configuration between the DL and the net moment of the AFi is reflected by the higher resistive state of the junction. For fields lower than -100 Oe, the DL remains in a single domain state, saturated along the negative field direction. The resistance of the junction for fields lower than this value is only modulated by the magnetization configuration in the AFi.

By further decreasing the negative applied magnetic field, the AFi net magnetic moment reverse by rotation of magnetizations in each layer leading to a decrease of the MTJ resistance. When the reversal of the net moment is completed [Fig. 1, state (3)], the magnetization of the AFi topmost layer becomes again parallel with the DL. However, since the two AFi layers rotate by 180° for the reversal of the net AFi moment, creation and annihilation of 360° domain walls in both thick and thin magnetic layers have been shown to appear.[5] In this field range, the intermediate reversal states [Fig. 1, states (1) and (2)] are constituted by multidomain configurations as shown by magnetic force microscopy (MFM) measurements. The MFM images illustrate how the wall structure starts to form [Fig. 1(b), state 1], how 360° walls are stabilized when domains completely reverse

a)Electronic mail: tiusan@ipcms.u-strasbg.fr

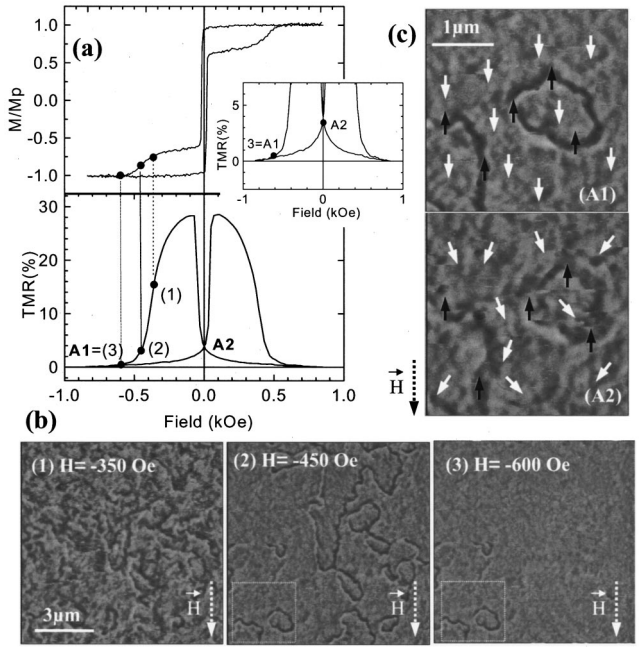

FIG. 1. (a) $M-H$ and TMR$-H$ curves for a Co/Ru/CoFe AFi based MTJ. States (1)–(3) define significant magnetization configurations during the AFi magnetization reversal. These configurations are illustrated by the associated MFM images (b) *state 1*: domain magnetization reversed by about 90°, the TMR reaches half of its maximum value, MFM wall contrast becomes enhanced; *state 2*: domain reversal is completed, stable domain wall structure is clearly resolved by MFM; *state 3* domain walls are almost annihilated, only isolated very stable walls persist. Inset: Zoom on the TMR$-H$ curve corresponding to low resistance range. (c) MFM images illustrating relaxation of magnetization in domains due to local anisotropies in the polycrystalline layers when reducing the external field from -600 Oe to zero. The Arrows sketch domain and domain wall magnetization orientation with respect to the external field.

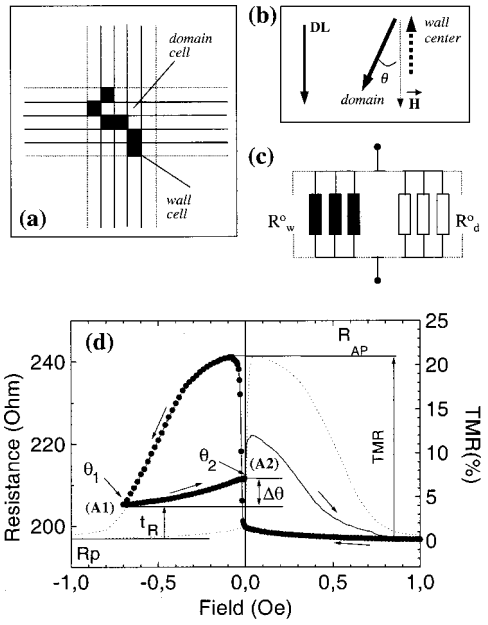

FIG. 2. Model for a MTJ in a multidomain state. (a) Elementary grid dividing the surface of the junction in elementary domain and wall cells. (b) Sketch illustrating magnetization orientation in a domain (straight arrow) and a domain wall (bold dotted arrow) with respect to the field direction in an intermediate state during the AFi net moment reversal. (c) Electrical model for the MTJ in a multidomain configuration: network of in-cascade resistances, corresponding to domain and domain wall associated tunneling paths. (d) Typical TMR$-H$ curve containing the main parameters used in our analytical model: $t_R(H)$, TMR, R_P, and R_{AP}. Legend: (·····): symmetric TMR loop taken in a field range where the domain reversal is completed ($t_R=0$); (-·-): ''minor'' TMR loop where the reversal in negative field in state (A1) is not yet completed ($t_R^{A1}\neq 0$).

along the field direction (state 2) and how the walls are annihilated at high fields (state 3). The MFM images shown in Figure 1(c): states (A1), (A2) illustrate the magnetization relaxation processes inside domains when reducing the negative fields from state A1 to A2.

In order to proceed to a quantitative analysis of the domain wall contribution to the tunnel magnetoresistance response, we have developed an analytical model which can be applied to junctions in a multidomain configuration. The total surface S of the junction is divided in a grid of n_w elementary wall cells and n_d elementary domain cells, each cell having an elementary surface s_0 [see Fig. 2(a)]. The total surface occupied by the walls is $S_w=n_w\times s_0$ whereas the total surface occupied by the domains is $S_d=n_d\times s_0$.

As discussed previously, during the magnetization reversal of the AFi, 360° domain walls are created.[5] The center of these walls is constituted by regions which magnetization remains blocked along the initial positive saturation direction, antiparallel to the DL, whereas the magnetization of adjacent domains makes an angle θ with respect to the external field direction and so to the DL. Assuming that in this field window the DL is in a single domain state, the resistance of the conduction channels associated to elementary domain R_d^0 and elementary wall R_w^0 cells is calculated as a function of the total resistance of the MTJ corresponding to perfect parallel R_P and antiparallel R_{AP} magnetic configurations:[5]

$$R_d^0=\frac{1}{2}\frac{S}{s_0}[R_P+R_{\mathrm{AP}}+(R_P-R_{\mathrm{AP}})\cos\theta]. \tag{1}$$

In this model, the center of the 360° wall is considered as a small ''domain'' of inverse magnetization. Tail related effects, when taking into account an analytical wall profile, are included in the angle θ which quantifies the average angle of the wall adjacent magnetization of the domain. Therefore, the resistance of the elementary wall can be written as:

$$R_w^0=\frac{S}{s_0}R_{\mathrm{AP}}. \tag{2}$$

The total resistance R of the MTJ in a multidomain configuration can be calculated as the equivalent resistance of a network of in-cascade resistances associated to domain, respectively domain wall elementary segments [Fig. 2(c)].

$$\frac{1}{R}=\sum_i\frac{1}{R_w^0}+\frac{1}{R_d^0}=\frac{n_w}{R_w^0}+\frac{n_d}{R_d^0} \tag{3}$$

$$=\frac{1}{s_0}\left[\frac{S_w}{R_w^0}+\frac{S-S_w}{R_d^0}\right]. \tag{4}$$

Lets consider the successive intermediate state occurring during the magnetization reversal [i.e., state (A1), Fig. 2(d)].

Here, the residual domain wall structure subsisting in the hard subsystem is reflected by the higher resistive state of the MTJ than the one corresponding to the perfect parallel configuration. Indeed, the center of the residual 360° walls being oriented opposite to the detection layer [see Fig. 2(b)] gives rise to high resistance tunneling channels, compared with tunneling channels associated to adjacent domains (low resistance). This high resistive state is ''quantified'' by a residual magnetoresistance t_R^{A1} and so a resistance $R(A1)$:

$$R(A1)=R_P(1+t_R^{A1}). \tag{5}$$

From Eq. (1)–(4), we can write:

$$\frac{1}{R_P(1+t_R^{A1})} = \frac{1}{s_0}\left[\frac{s_0}{S}\frac{S_w^{A1}}{R_{AP}}+\frac{2s_0(S-S_w^{A1})/S}{(R_P+R_{AP}+(R_P-R_{AP})\cos\theta^{A1}}\right]. \tag{6}$$

Using the definition of the tunnel magnetoresistance: $TMR=(R_{AP}-R_P)/R_P$, one can deduce from the Eq. (6), the surface of the walls with respect to the total surface of the junction responsible for a residual magnetoresistance t_R^{A1}:

$$\omega^{A1}=\frac{S_w^{A1}}{S}=\frac{t_R^{A1}-\dfrac{TMR(1-\cos\theta^{A1})}{2}}{\dfrac{TMR(1+\cos\theta^{A1})}{2}}\frac{1+TMR}{1+t_R^{A1}}. \tag{7}$$

From state (A1) when decreasing the field towards zero, the resistance of the junction increases to state (A2). Since ω remains unchanged when the magnetic field is decreased, the variation of the MTJ resistance is only related to the relaxation of the magnetization in the domains as shown in the MFM images of Fig. 1(c). Here again, the variation of the wall profile with the field, such as tails effects for instance, are included in the angle θ of wall adjacent domain magnetization. By measuring the residual t_R^{A2} from the TMR curve, one can calculate the angle of domain magnetization θ^{A2} corresponding to a given density of domain walls ω^{A1}.

$$\cos\theta^{A2}=\frac{t_R^{A2}-\dfrac{TMR}{2}\left[\omega^{A1}\dfrac{1+t_R^{A2}}{1+TMR}+1\right]}{\dfrac{TMR}{2}\left[\omega^{A1}\dfrac{1+t_R^{A2}}{1+TMR}-1\right]}. \tag{8}$$

This equation, applied for the states (A1) and (A2), gives the relaxation angle

$$\Delta\theta=\theta^{A2}-\theta^{A1}. \tag{9}$$

This analytical model is used for quantitative analysis of the AFi magnetization reversal, illustrated by the (1)–(2)–(3) branch of the $M-H$ and TMR$-H$ curves in Fig. 1. As shown by MFM measurements, in states (2) or (3), the domain magnetization is practically reversed ($\theta\simeq 0$) but domain wall structure persist ($\omega\neq 0$). From the residual magnetoresistance t_R in a given state and considering $\theta=0$, the density of walls (ω) can be calculated from Eq. (7). In state (2) of Fig. 1, the calculated residual density of walls is $\omega\simeq 17.2\%$ corresponding to a residual $t_R\simeq 4\%$ and a TMR$=28.8\%$. This value becomes slightly smaller (15.3%) when considering a contribution of magnetization angle in domains described by an angle $\theta=15°$. These values are in good agreement with the value extracted from analysis of the MFM image Fig. 1(b), state (2), $\omega_{MFM}\simeq 15\%$. Similar analysis performed for state (3) of Fig. 1 gives values for the density of walls $\omega\simeq 2\%$ for $t_R=0.5\%$. This result is also in good agreement with the value extracted from the MFM image analysis. The relaxation of domain magnetization, reflected by the increase in the junction resistance between the states (3)$=$(A1) and (A2) Fig. 1(a) and illustrated by the MFM images of Fig. 1(c), is quantified using the set of Eqs. (8) and (9). Indeed, between the state (A1) defined by $t_R^{A1}=0$ and $\theta^{A1}=0$, and the state (A2) ($H=0$ Oe) defined by $t_R^{A2}=3.4\%$, we estimate a relaxation angle of $\Delta\theta\simeq 38°$ when reducing the field. The extracted value quantifies the local anisotropy distribution in the AFi layers, key factor in magnetization reversal of a polycrystalline system.[5]

In conclusion, a good agreement is found between results extracted from the TMR analysis and the data extracted from the analysis of the MFM images. This suggest that the analytical model used for this study and adapted to tunnel junctions in a multidomain state, is a useful tool to quantify both domain wall density and local anisotropy distributions.

The authors are grateful for illuminating discussions with H. van den Berg, V. da Costa, and experimental support of C. Meny, Y. Henry, M. Acosta, and G. Wurz. This work was supported by the European Framework IV Materials Technology Programme, Contract No. BRPR-CT98-0657, the *Dynaspin* program, *Training and Mobility of Researchers* network, under Contract. No. FMRX-CT97-0147 and the Nanomem Program (IST-1999-13741). One of the authors (K.O.) also acknowledges NSF Grant No. CNRS-9603252.

[1] S. Gider, B.-U. Runge, A. C. Marley, and S. S. P. Parkin, Science **281**, 797 (1998).
[2] K. S. Moon, R. E. Fontana, and S. S. P. Parkin, Appl. Phys. Lett. **74**, 3690 (1999).
[3] A. Anguelouch, B. Shrang, G. Xiao, Y. Lu, P. Trouilloud, W. J. Gallagher, and S. S. P. Parkin, Appl. Phys. Lett. **76**, 622 (2000).
[4] L. Thomas, M. G. Samant, and S. S. P. Parkin, Phys. Rev. Lett. **84**, 1816 (2000).
[5] C. Tiusan, T. Dimopoulos, K. Ounadjela, M. Hehn, H. A. M. van den Berg, Y. Henry, and V. Da Costa, Phys. Rev. B **61**, 580 (2000).
[6] M. Hehn, O. Lenoble, D. Lacour, C. Fery, M. Piecuch, C. Tiusan, and K. Ounadjela, Phys. Rev. B **61**, 11643 (2000).
[7] C. Tiusan, M. Hehn, K. Ounadjela, Y. Henry, J. Hommet, C. Meny, H. A. M. van den Berg, L. Baer, and R. Kinder, J. Appl. Phys. **8**, 5276 (1999).